

Microwave absorption of mixed-layer transition metal dichalcogenides

K. Hayashi^{a,*}, D. Serikawa^a, Y. Chijimatsu^a, M. Shimakawa^a, S. Kume^a,
K. Manabe^a, T. Takahashi^b

^aLaboratory for Solid State Chemistry, Okayama University of Science, 1-1 Ridai-cho, Okayama 700, Japan

^bNKK corporation, 1 Kokan-cho, Fukuyama 721, Japan

Abstract

'Mixed-layer mechanism', a new concept in microwave absorption, was observed in mixed-layer transition-metal dichalcogenides. Two things were observed: first, the strong microwave absorption in the mixed-layer transition metal dichalcogenides, $M_xM'_{1-x}ch_2$ ($M = \text{Re, Ru and Os}$; $M' = \text{Nb and Ta}$; $ch = \text{S and Se}$); second, the low microwave absorption in the nominally-perfect stacking $3R\text{-MoS}_2$ and $M_xM'_{1-x}ch_2$ ($M = \text{Re, Ru and Os}$; $M' = \text{Nb and Ta}$; $ch = \text{S and Se}$). © 1997 Elsevier Science S.A.

Keywords: Layered-transition metal dichalcogenide; Mixed-layer structure; Microwave absorption; Structure-property relation

1. Introduction

The energy of a microwave is around 0.0001 eV and the microwave absorption is observed in simple molecular gases, with the transitions between the rotational energy levels being responsible for microwave absorption [1]. Three kinds of electromagnetic wave absorption mechanisms in solid compounds have been considered: (a) dielectric-loss mechanism [2]; (b) magnetic hysteresis-loss mechanism [3]; and (c) conduction-loss mechanism [2]. Electromagnetic absorption by the magnetic hysteresis-loss mechanism occurs in the low and broad band; the dielectric-loss mechanism occurs in the high-frequency band; and the conduction-loss mechanism occurs in the narrow band.

The magnetic hysteresis-loss originates in the motion and friction of the magnetic domain wall, the dielectric loss in the motion of the ferroelectric domain wall and the conduction-loss in the electron scattering. The typical electromagnetic absorption materials of the dielectric loss mechanism, the magnetic hysteresis loss mechanism and the conduction loss mechanism are barium titanate, ferrite and graphite or metal powder, respectively. The graphite material is the best of the three and absorbs the microwave of 2.45 GHz 10 times more than the others. From the quantum mechanical point of view, the electron transition between the band gap corresponding to the microwave frequency causes the microwave absorption. If there are many non-degenerate energy levels around the microwave energy, microwave absorption will occur in the broad band. We have researched such a system in the random-structure-compounds. Recently, we found mixed-layer structure in a

* Corresponding author.

series of the transition metal dichalcogenides, $\text{Re}_x\text{Ta}_{1-x}\text{Se}_2$ and $\text{Os}_x\text{Ta}_{1-x}\text{Se}_2$ [4].

In the present investigation, the mixed-layer compounds, $\text{Ru}_x\text{Nb}_{1-x}\text{S}_2$, $\text{Re}_x\text{Nb}_{1-x}\text{S}_2$, $\text{Ru}_x\text{Nb}_{1-x}\text{Se}_2$, $\text{Re}_x\text{Nb}_{1-x}\text{Se}_2$, $\text{Os}_x\text{Nb}_{1-x}\text{Se}_2$ and $\text{Os}_x\text{Ta}_{1-x}\text{Se}_2$, were prepared and the microwave absorption of these mixed-layer compounds were measured. High microwave absorption was observed in the mixed-layer compounds, and the correlation between the mixed-layer structure and the relative microwave absorption coefficient is discussed.

2. Experimental

2.1. Preparation and simulation of powder X-ray diffraction

The samples were prepared by the conventional vacuum sealed method [4] and crystal structures were analyzed by the Rietveld method with the computer program RIETAN [5]. The simulations of the powder X-ray diffraction patterns of mixed-layer structures were performed with the program SEKITAN [4].

2.2. Measurement of microwave absorption

The microwave absorption measurement of 2.45 GHz was performed with the apparatus shown in Fig. 1. The microwave source is a 300-W magnetron, the temperature of the sample was monitored with a pyrometer and the sample is set on the microwave-transparent silica glass plate. The heating rate of the sample is represented by the equation:

$$T = T_0 + \frac{\mu H}{\alpha} \left\{ 1 - \exp\left[-\frac{\alpha}{C_p} t\right] \right\} \quad (1)$$

where T is a sample temperature; T_0 is room temperature; μ is a relative microwave absorption coefficient; H is an intensity of the microwave source; α is thermal radiation; C_p is heat capacity; and t is time. In the stationary state, Eq. (1) was simplified into Eq. (2):

$$T = T_0 + \frac{\mu H}{\alpha} \quad (2)$$

The sample temperature was saturated after a long duration of time. The divergence at the starting point was a function of the heat capacity, the intensity of the microwave source and the relative microwave absorption coefficient are as shown in Eq. (3):

$$\frac{dT}{dt} = \frac{\mu H}{C_p} \quad (3)$$

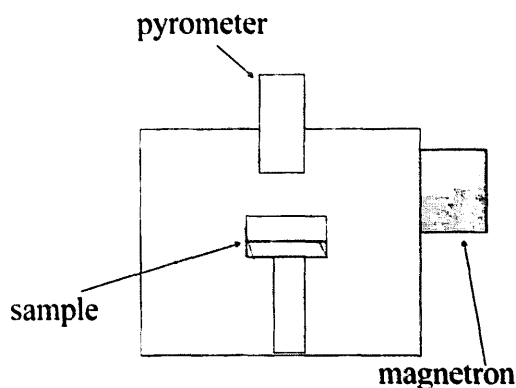


Fig. 1. Schematic diagram of apparatus for measuring microwave absorption.

The relative microwave absorption coefficient was obtained according to Eq. (3) if the divergence at the starting point of the sample was compared with that of the reference material. In the present investigation, iron powder of 20 mesh was used for the reference material of the microwave absorption coefficient. The microwave absorption coefficient of the reference iron powder was defined as one.

3. Results and discussion

3.1. NbS_2 - RuS_2 system

The phase diagram and the microwave absorption coefficient of the compounds in the NbS_2 - RuS_2 system are shown in Fig. 2. The mixed-layer phase was stabilized around 10 mol% RuS_2 . Two two-phase regions existed within the composition range.

The relative microwave absorption coefficient

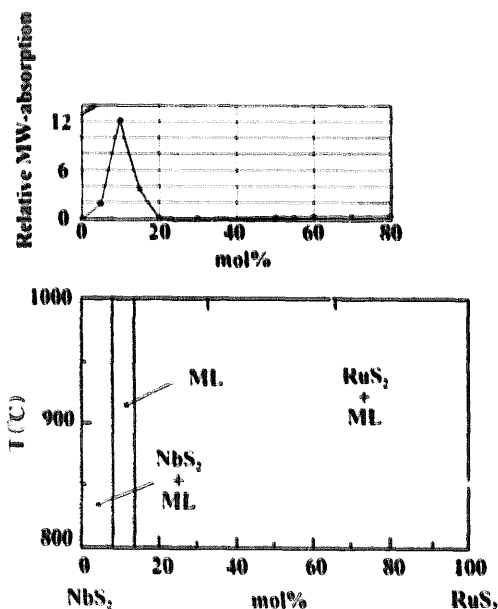


Fig. 2. Microwave absorption of the compounds in NbS_2 - RuS_2 system. *Absorption coefficient is normalized by the reference iron powder; ML: mixed layer phase.

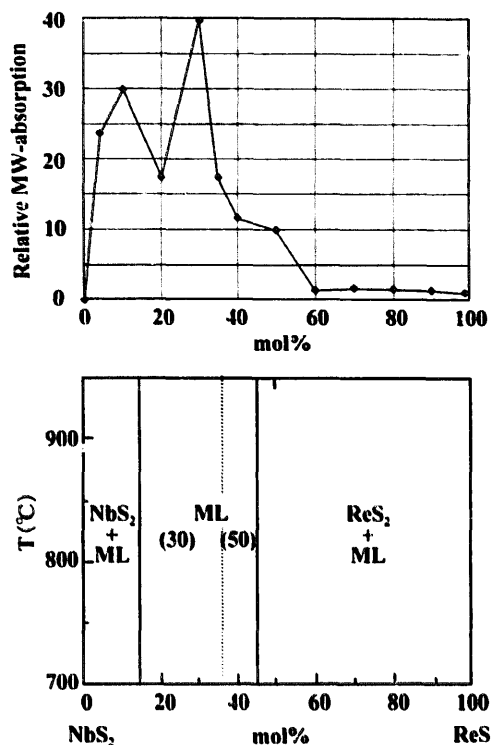


Fig. 3. Microwave absorption of the compounds in NbS_2 - ReS_2 system. *Absorption coefficient is normalized by the reference iron powder; ML: mixed layer phase.

showed a maximum value of 12.1 at the 10 mol% RuSe_2 and rapidly dropped to nearly zero value above and below 10 mol% RuSe_2 . The composition of the maximum microwave absorption coincided with the composition of the mixed-layer structure.

3.2. NbS_2 - ReS_2 system

The phase diagram and the microwave absorption coefficient of the compounds in the NbS_2 - ReS_2 system are shown in Fig. 3. The mixed-layer phase was stabilized in the composition range between 13 mol% ReS_2 and 45 mol% ReS_2 . The mixed-layer structure in the composition ranged between 13 mol% ReS_2 and 36 mol% ReS_2 was constructed with $2H_b$ -slabs of 30% and $3R$ -slabs of 70%, while the mixed-layer structure in the range between 36 mol% ReS_2 and 45 mol% ReS_2 was constructed with $2H_b$ -slabs of 50% and $3R$ -slabs of 50%. Two two-phase regions existed within the composition range.

The relative microwave absorption coefficient showed two maximum values: 30 and 40 at the compositions of 10 mol% ReS_2 and 30 mol% ReS_2 , respectively. The highest value was attained by the mixed-layer phase and the second maximum value arose from the mixture of the mixed-layer phase and NbS_2 phase. However, the values of the relative microwave absorption of the samples were higher than

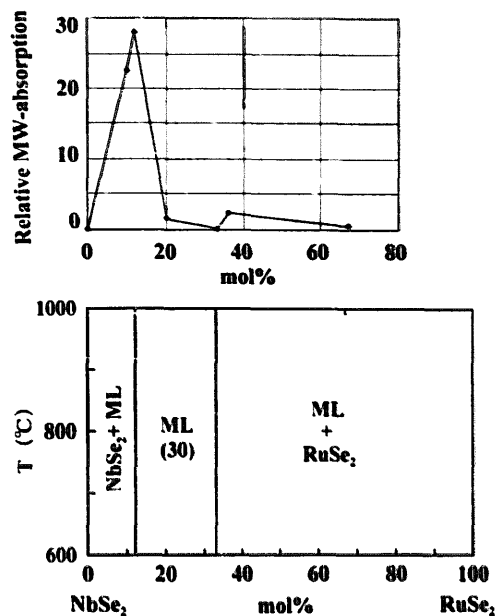


Fig. 4. Microwave absorption of the compounds in NbSe_2 - RuSe_2 system. *Absorption coefficient is normalized by the reference iron powder; ML: mixed layer phase.

10 in the mixed-layer phase and rapidly decrease down to nearly zero in the two-phase region.

3.3. NbSe_2 - RuSe_2 system

The phase diagram and the microwave absorption coefficient of the compounds in the NbSe_2 - RuSe_2 system are shown in Fig. 4. The mixed-layer phase was stabilized in the composition range between 12 mol% RuSe_2 and 33 mol% RuSe_2 . The structure of the mixed-layer phase in this system was constructed with $2H_b$ -slabs of 30% and $3R$ -slabs of 70%. Two two-phase regions existed within the composition range.

The relative microwave absorption coefficient showed a maximum value of 28 at the composition of 12 mol% RuSe_2 and rapidly dropped to nearly zero value above and below 12 mol% RuSe_2 . The composition of the compound at this maximum microwave absorption coincides with the composition of the compound of the mixed-layer structure. The mixture of the mixed-layer phase and NbSe_2 phase also showed a high microwave absorption value.

3.4. NbSe_2 - ReSe_2 system

The phase diagram and the microwave absorption coefficient of the compounds in the NbSe_2 - ReSe_2 system are shown in Fig. 5. The mixed-layer phase was stabilized in the composition range between 12 mol% ReSe_2 and 50 mol% ReSe_2 . The structure of the mixed-layer phase in this system was constructed

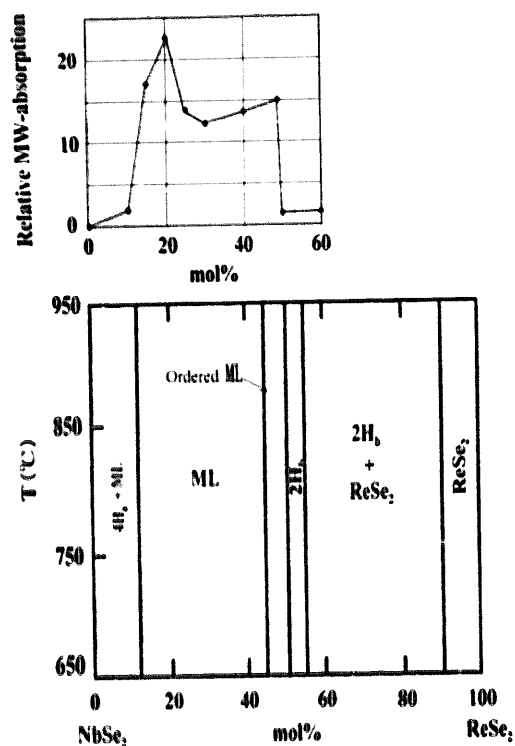


Fig. 5. Microwave absorption of the compounds in NbSe_2 - ReSe_2 system. *Absorption coefficient is normalized by the reference iron powder; ML: mixed layer phase.

with $2H_b$ -slabs of 30% and $3R$ -slabs of 70%. The $2H_b$ - $\text{Re}_x\text{Nb}_{1-x}\text{Se}_2$ phase appears in the composition range between 50 mol% ReSe_2 and 55 mol% ReSe_2 . Two two-phase regions existed within the composition range.

The relative microwave absorption coefficient showed two maximum values, 23 and 15 at the compositions of 20 mol% ReSe_2 and 50 mol% ReSe_2 , respectively. The highest value was attained by the mixed-layer phase and the second maximum value was also reached by the mixed-layer phase. The values of the relative microwave absorption of the samples were higher than 15 in the mixed-layer phase and rapidly decreased down to nearly zero in the two-phase region.

3.5. NbSe_2 - OsSe_2 system

The phase diagram and the microwave absorption coefficient of the compounds in the NbSe_2 - OsSe_2 system are shown in Fig. 6. The mixed-layer phase was stabilized in the composition range between 10 mol% OsSe_2 and 33 mol% OsSe_2 . There are four mixed-layer compositions. The first one ranged between 10 mol% OsSe_2 and 22 mol% OsSe_2 and was constructed with $2H_b$ -slabs of 30% and $3R$ -slabs of 70%. The second composition ranges between 22 mol% OsSe_2 and 27 mol% OsSe_2 , with $2H_b$ -slabs of

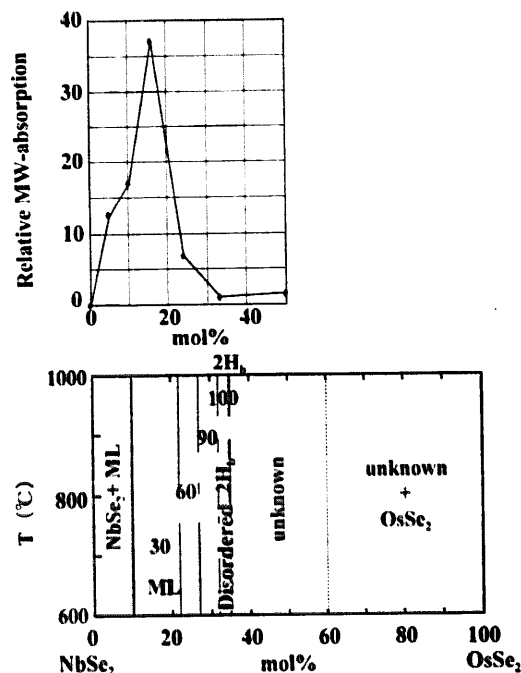


Fig. 6. Microwave absorption of the compounds in NbSe_2 - OsSe_2 system. *Absorption coefficient is normalized by the reference iron powder; ML: mixed layer phase.

60% and $3R$ -slabs of 40%. The third one ranged between 27 mol% OsSe_2 and 33 mol% OsSe_2 , with $2H_b$ -slabs of 90% and $3R$ -slabs of 10%. The fourth composition, the disordered $2H_b$ - $\text{Os}_x\text{Nb}_{1-x}\text{Se}_2$ phase, constructed with the $2H_b$ -slabs of 100% lay in the composition range between 33 mol% OsSe_2 and 35 mol% OsSe_2 . In addition to the four composition ranges, there was also an unknown phase, possibly a new mixed-layer phase, which appeared in the composition range between 35 mol% OsSe_2 and 60 mol% OsSe_2 . Two two-phase regions existed within the composition range.

The relative microwave absorption coefficient showed a maximum value of 37 in the composition of 16 mol% OsSe_2 and rapidly dropped to nearly zero value below and over this value. The composition of the compound of this maximum microwave absorption coincided with the composition of the compound of the mixed-layer structure. The mixture of the mixed-layer phase and NbSe_2 phase also showed a high microwave absorption value.

3.6. TaSe_2 - OsSe_2 system

The phase diagram and the microwave absorption coefficient of the compounds in the TaSe_2 - OsSe_2 system are shown in Fig. 7. The mixed-layer phase was stabilized in the composition range between 10 mol% OsSe_2 and 31 mol% OsSe_2 . There were three composition ranges. The first one ranges between 10 mol% OsSe_2 and 15 mol% OsSe_2 and was con-

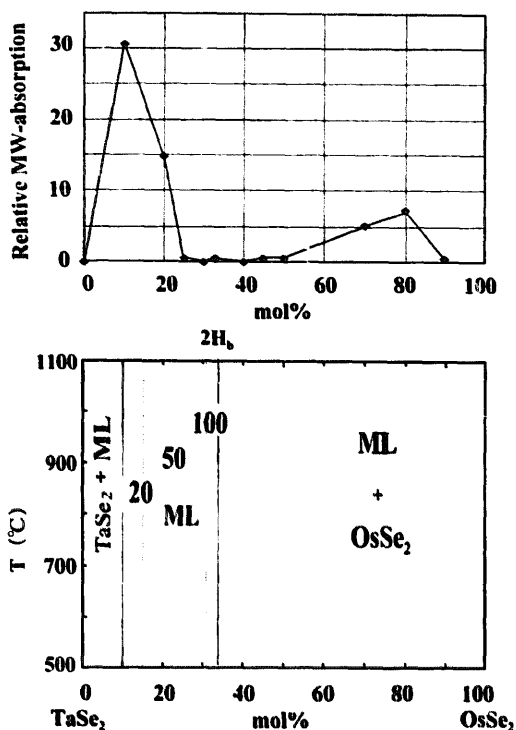


Fig. 7. Microwave absorption of the compounds in TaSe₂-OsSe₂ system. *Absorption coefficient is normalized by the reference iron powder; ML: mixed layer phase.

structured with 2H_b-slabs of 20% and 3R-slabs of 80%. The second composition ranged between 15 mol% OsSe₂ and 31 mol% OsSe₂, with 2H_b-slabs of 50% and 3R-slabs of 50%. The third one, the disordered 2H_b-Os_xTa_{1-x}Se₂ phase constructed with 2H_b-slabs of 100%, lay in the composition range between 31 mol% OsSe₂ and 33 mol% OsSe₂. Two two-phase regions existed within the composition range.

The relative microwave absorption coefficient showed two maximum values: the high maximum value of 32 at the composition of 10 mol% OsSe₂ and the low maximum value of seven at the composition of 80 mol% OsSe₂. This coefficient rapidly dropped to nearly zero value above and below the high maximum value. The composition of the compound of the high maximum microwave absorption coincided with the composition of the compound of the mixed-layer structure. The low maximum absorption value was from the mixture of the disordered 2H_b-Os_xTa_{1-x}Se₂ phase and OsSe₂ phase. However, the values of the microwave absorption of the mixed-layer phase were higher than those of the two-phase.

3.7. *d*⁵-*d*⁷ dichalcogenide system

The NbS₂-ReS₂ system and the NbSe₂-ReSe₂ system are summarized as the *d*⁵-*d*⁷ dichalcogenide system.

The composition range of the mixed-layer phase of

the *d*⁵-*d*⁷ dichalcogenide system was generally wide and lay between approx. 10 mol% *d*⁷-dichalcogenide and approx. 50 mol% *d*⁷-dichalcogenide. The microwave absorption coefficient showed two maximum values with the high maximum value being attained by the mixed-layer phase. The microwave absorption coefficient of the mixed-layer phase was generally higher than that of the other phase.

3.8. *d*⁵-*d*⁸ dichalcogenide system

The NbS₂-RuS₂ system, the NbSe₂-RuSe₂ system, NbSe₂-OsSe₂ system and the TaSe₂-OsSe₂ system are summarized as the *d*⁵-*d*⁸ dichalcogenide system.

The composition range of the mixed-layer phase of the *d*⁵-*d*⁸ dichalcogenide system was narrower than that of the *d*⁵-*d*⁷ dichalcogenide system and lay between approx. 10 mol% *d*⁸-dichalcogenide and approx. 33 mol% *d*⁸-dichalcogenide. The microwave absorption coefficient showed generally one maximum value, this value being attained by the mixed-layer phase. The microwave absorption coefficient of the mixed-layer phase was generally higher than that of the other phase.

4. Conclusions

The relative microwave absorption of 2.45 GHz is estimated by measuring the rising sample-temperature during radiation, with iron powder being used as a standard substance. The microwave absorption of the nominally-perfect stacking 3R-MoS₂ is very low and undetectable. The microwave absorption of the mixed-layer compounds, Re_{0.15}Nb_{0.85}Se₂ and Os_{0.16}Nb_{0.84}Se₂, is high. However, that of the normal stacking compounds, Re_{0.5}Nb_{0.5}Se₂ and Os_{0.33}Nb_{0.67}Se₂, is as low as that of the standard iron powder. The microwave absorption of the 2H_b-NbSe₂ and the 3R-NbSe₂ is as low as that of the MoS₂. These results suggest that the microwave absorption of the transition metal dichalcogenides depends on the layer stacking. The microwave absorption increases as the disorder of the layer stacking of the compounds increases while that of the perfect-stacking compounds is very low and undetectable.

These transition metal dichalcogenides show the behavior of metals or semiconductors. The mixed-layer minerals are insulators and show the lower microwave absorption coefficients.

In conclusion, the microwave absorption of the layered compounds is strongly dependent on the crystal structure, especially layer stacking. The electrical conductivity of the layered compounds is also an important factor for inducing microwave absorption.

The present results indicate that the mixed-layer

structure reveals many non-degenerate energy levels around the microwave energy and that strong microwave absorption will occur in the broad band.

Acknowledgements

Part of the present research was supported by a grant-aid from the NKK Co. Japan. The author would like to thank Mr. Matthew Main for reading the manuscript and giving us advice about English expressions.

References

- [1] C.H.Townes, A.L. Schawlow, *Microwave Spectroscopy*, Dover, New York, 1975, pp. 613–642.
- [2] R.E. Newnham, S.J. Jang, M. Xu, F. Jones, *Ceram. Trans.* 21 (1991) 51–67.
- [3] S.Chikazumi, *Physics of Magnetism*, Wiley, New York, 1964, pp. 202–253.
- [4] K. Hayashi, T. Ikeuchi, H. Takauchi, M. Shimakawa, *J. Alloys Comp.* 219 (1995) 161–167.
- [5] F. Izumi, *J. Cryst. Jpn.* 27 (1985) 23.